A Structural Determinant of the Unique Interfacial Binding Mode of Bovine Pancreatic Phospholipase A_2[†]

Byung In Lee, Rajiv Dua,[‡] and Wonhwa Cho*

Department of Chemistry (M/C 111), University of Illinois at Chicago, 845 West Taylor Street, Chicago, Illinois 60607-7061

Received March 16, 1999; Revised Manuscript Received April 22, 1999

ABSTRACT: The catalytic steps of the phospholipase A_2 (PLA_2)-catalyzed hydrolysis of phospholipids are preceded by interfacial binding. Among various pancreatic PLA_2s, bovine pancreatic PLA_2 ($bpPLA_2$) has a unique interfacial binding mode in which Lys-56 plays an important role in its binding to anionic lipid surfaces. To identify the structural determinant of this unique interfacial binding mode of $bpPLA_2$, we systematically mutated $bpPLA_2$ and measured the effects of mutations on its interfacial binding and activity. First, different cationic clusters were generated in the amino-terminal α-helix by the N6R, G7K, and N6R/G7K mutations. These mutations enhanced the binding of $bpPLA_2$ to anionic liposomes up to 15-fold. For these mutants, however, the K56E mutation still caused a large drop in interfacial affinity for and activity toward anionic liposomes, indicating that the generation of a cationic patch in the amino-terminal α-helix of $bpPLA_2$ did not change its interfacial binding mode. Second, residues 62−66 that form a part of the pancreatic loop were deleted. For this deletion mutant (Δ^{62-66}), which was as active as wild-type toward anionic liposomes, the K56E and K116E mutations (Δ^{62-66}/K56E and Δ^{62-66}/K116E) did not have significant effects on interfacial affinity. In contrast, the K10E mutation showed a much larger decrease in interfacial affinity (10-fold), indicating the deletion of residues 62−66 caused a major change in the interfacial binding mode. Finally, hydrophobic residues in positions 63 and 65 were replaced by bulkier ones (V63F and V63F/V65L) to pinpoint the structural determinant of the interfacial binding mode of $bpPLA_2$. The effects of K10E and K56E mutations on the interfacial affinity and activity of these mutants showed that Val-63 and Val-65 of $bpPLA_2$ are the structural determinant of its unique interfacial binding mode and that relatively conservative substitutions at these positions result in large changes in the interfacial binding mode among mammalian pancreatic PLA_2s. Taken together, this study reveals how minor structural differences among homologous PLA_2s can lead to distinct interfacial binding behaviors.

Phospholipase A_2 (PLA_2; EC 3.1.1.4)[1] catalyzes the hydrolysis of the fatty acid ester in the 2-position of 3-*sn*-phospholipids and is found in both intracellular and secreted forms (*1*−*5*). Secretory PLA_2s are small proteins (14−16 kDa) that can be classified into several groups based on structural differences (*6*). The structural (*4*, *7*) and mutational (*8*−*12*) analyses of several secretory PLA_2s have indicated that they have an interfacial binding surface (IBS) that is topologically distinct from the active site. The putative IBS of secretory PLA_2 is located on a flat molecular surface which contains several hydrophobic residues and cationic residues. However, questions still remain as to which forces drive the interfacial binding of individual secretory PLA_2s, which protein residues are essential for their interfacial binding, and whether different secretory PLA_2s have similar or distinct interfacial binding residues. The preceding report shows that even among highly homologous mammalian pancreatic PLA_2, there are major differences in the way they interact with lipid aggregates. For porcine ($ppPLA_2$) and human pancreatic PLA_2 ($hpPLA_2$), cationic residues in the amino-terminal region and Lys-116 in the carboxy terminus are important for their interfacial binding. For bovine pancreatic PLA_2 ($bpPLA_2$), however, Lys-56, in addition to Lys-10 and Lys-116, play essential roles in interfacial binding (*8*). To identify a structural determinant of this unique interfacial binding mode of $bpPLA_2$, we systematically mutated $bpPLA_2$ based on minor structural differences among these pancreatic PLA_2s. Herein, we present the kinetic and liposome binding data of these mutants which lead to the identification of the structural determinant of the unique interfacial binding mode of $bpPLA_2$.

MATERIALS AND METHODS

Materials. 1,2-Dihexanoyl-*sn*-glycero-3-phosphocholine (diC_6PC) and 1,2-dioctanoyl-*sn*-glycero-3-phosphocholine

[†] This work was supported by grants from National Institutes of Health (GM52598 and GM53987). W.C. is an Established Investigator of the American Heart Association.

* To whom correspondence should be addressed. Telephone: 312-996-4883. Fax: 312-996-2183. E-mail: wcho@uic.edu.

[‡] Present address: 147-75CH, Braun Laboratories, California Institute of Technology, Pasadena, CA 91125.

[1] Abbreviations: BLPG, 1,2-bis[12-(lipoyloxy)dodecanoyl]-*sn*-glycero-3-phosphoglycerol; $bpPLA_2$, bovine pancreatic phospholipase A_2; CD, circular dichroism; diC_6PC, 1,2-dihexanoyl-*sn*-glycero-3-phosphocholine; diC_8PC, 1,2-dioctanoyl-*sn*-glycero-3-phosphocholine; $hpPLA_2$, human pancreatic phospholipase A_2; IBS, interfacial binding surface; PLA_2, phospholipase A_2; $ppPLA_2$, porcine pancreatic phospholipase A_2; pyrene-PG, 1-hexadecanoyl-2-(1-pyrenedecanoyl)-*sn*-glycero-3-phosphoglycerol; SDS, sodium dodecyl sulfate.

10.1021/bi9906017 CCC: $18.00
Published on Web 05/26/1999

(diC_8PC) were purchased from Avanti Polar Lipids (Alabaster, AL) and used without further purification. 1-Hexadecanoyl-2-(1-pyrenedecanoyl)-*sn*-glycero-3-phosphoglycerol (pyrene-PG) was obtained from Molecular Probes (Eugene, OR). 1,2-Bis[12-(lipoyloxy)dodecanoyl]-*sn*-glycero-3-phosphoglycerol (BLPG) was prepared as described previously (*13*). Large unilamellar liposomes were prepared by multiple extrusion through a 0.1-μm polycarbonate filter in a Liposofast microextruder (Avestin; Ottawa, Ontario). Phospholipid concentrations were determined by phosphate analysis (*14*). Fatty acid-free bovine serum albumin, guanidinium chloride, and *n*-dodecanoylsucrose were from Miles Inc. (Kankakee, IL), Fisher, and Calbiochem (San Diego, CA), respectively. All the restriction enzymes, T4 ligase, T4 polynucleotide kinase, and isopropyl β-D-thiogalactopyranoside were obtained from Boehringer Mannheim Biochemicals. Oligonucleotides were purchased from Integrated DNA Technologies (Coralville, IA).

Construction of Mutant Phospholipase A_2 Genes. The site-directed mutagenesis of $bpPLA_2$ was performed using the M13mp18 vector containing $bpPLA_2$ gene according to the method of Eckstein (*15*) using an in vitro mutagenesis kit from Amersham−Pharmacia. To enhance the efficiency of mutation, multiple mutations, e.g., N6R/G7K/K56E, were performed sequentially. The oligonucleotides used for the construction of mutants were 5′-GAT CAT TCC ACG AAA CTG CCA-3′ (N6R), 5′-ACA TTT GAT CAT TTT GTT AAA CTG CCA-3′ (G7K), 5′-GAT CAT TTT ACG AAA CTG-CCA-3′ (N6R/G7K), 5′-TCT TAC ATT CGA TCA TTC C-3′ (K10E), 5′-ATC AAG TTT TTC AGC TTG TT-3′ (K56E), 5′-GTT ATT TGT ATA CGG ATT GCA GCT ATC AAG TTT TTT AGC TTG TTT ATA G-3′ (Δ62−66), 5′-T ATC AAG ATT TTC GTG TTC TT-3′ (K116E), 5′-G ATT GTS GAC AAG GAA TTT GCA GCT ATC-3′ (V63F), and 5′-TA CGG ATT GTC GAG AAG GAA TTT GCA GC-3′ (V63F/V65L), respectively, in which the underlined bases indicate the location of mutation(s). After the DNA sequences of mutants were verified by the sequencing analysis using a Sequenase 2.0 kit (Amersham−Pharmacia), individual recombinant $bpPLA_2$ genes were digested with *Eco*RI and *Bam*HI, and inserted into the pTO-propla2 vector (*16*) for protein expression.

Protein Expression and Purification. $bpPLA_2$ and its mutant proteins were expressed as inclusion bodies in an *Escherichia coli* strain, BL21(DE3)pLysS (Novagen, Madison, WI), using the pTO-propla2 vector as described (*8*). Briefly, the sulfonated proteins (ca. 10 mg) dissolved in 10 mL of 50 mM Tris-HCl, pH 8.0, containing 5 mM ethylenediaminetetraacetic acid and 8 M urea were slowly diluted with 30 mL of 50 mM Tris-HCl, pH 8.0, containing 8 mM reduced glutathione, 4 mM oxidized glutathione, and 5 mM ethylenediaminetetraacetic acid. The solution was kept at room temperature for 20 h, dialyzed against 50 mM ammonium bicarbonate, and lyophilized. The mature refolded proteins were then purified chromatographically using a HiLoad 16/10 S Sepharose column (Amersham−Pharmacia) attached to a FPLC system (Amersham−Pharmacia). The column was equilibrated in 10 mM ammonium acetate, pH 5.0, and eluted with a linear gradient of increasing NaCl concentration from 0 to 0.5 M in the same buffer. All the proteins were eluted as a major peak with the appropriate concentrations of NaCl. Fractions corresponding to the major protein peak were pooled, dialyzed against water, and lyophilized. The lyophilized proteins were stored at −20 °C. The purity of protein was confirmed by SDS−polyacrylamide electrophoresis. Protein concentrations were determined by the bicinchoninic acid method (Pierce). The circular dichroism (CD) spectra of proteins were measured in 10 mM phosphate buffer, pH 7.4, at 25 °C using a Jasco J-600 spectropolarimeter. Each spectrum was obtained at wavelengths between 200 and 300 nm and averaged from 10 separate scans.

Measurements of Protein Stability. The thermodynamic stability of wild-type and mutant proteins was measured from their equilibrium denaturation by guanidinium chloride. Briefly, the proteins were incubated in 10 mM phosphate buffer, pH 7.4, containing 0−8 M guanidinium chloride for 2 h at 23 °C and their CD spectra measured. Assuming that the protein folding follows the two-state model (i.e., native ↔ unfolded), the molar ellipticity values at 222 nm (θ_{222}) at different guanidinium chloride concentrations were converted to the fraction of unfolded protein (f_u) using the equation: $f_u = (\theta_N - \theta_{222})/(\theta_N - \theta_U)$ where θ_N and θ_U are extrapolated base lines for the native and unfolded protein, respectively (*17*, *18*). The free energy of folding (ΔG_{fold}) was determined from the nonlinear least-squares analysis of the f_u vs [guanidinium chloride] plot using the equation:

$$f_u = 1/\left\{1 + \exp\left(-\left[\frac{\Delta G_{fold}}{RT} + \frac{m[\text{guanidinium chloride}]}{RT}\right]\right)\right\}$$

where m indicates the slope of the plot in the transition region.

Kinetic Measurements. All kinetic experiments were performed at 37 °C. The PLA_2-catalyzed hydrolysis of polymerized mixed liposomes was carried out in 2 mL of 10 mM HEPES buffer, pH 7.4, containing 10 μM pyrene-PG/BLPG (1:99 in mole ratio) polymerized mixed liposomes, 2 μM bovine serum albumin, 0.16 M NaCl, and 10 mM $CaCl_2$. The progress of hydrolysis was monitored fluorometrically, and the rate constants were calculated from the nonlinear least-squares analysis of the reaction progress curves as described previously (*8*, *13*, *19*). The PLA_2-catalyzed hydrolysis of diC_6PC monomers and diC_8PC micelles was performed with 0.5 mM phospholipid, 0.16 M NaCl, and 10 mM $CaCl_2$. The time course of phospholipid hydrolysis was monitored with a computer-controlled Metrom pH stat (Brinkmann) in a thermostated vessel. Under these conditions, the hydrolysis of diC_6PC and diC_8PC followed first-order kinetics because the substrate concentrations remained lower than the apparent K_M values. Thus, the $(k_{cat}/K_m)_{app}$ values were calculated by dividing by the enzyme concentration the pseudo-first-order rate constants determined from the nonlinear least-squares analysis of reaction progress curves.

Liposome−Protein Binding Measurements. The binding of $bpPLA_2$ and mutants to sucrose-loaded polymerized liposomes was measured by a centrifugation method as described previously (*11*). For binding measurements, a given concentration of BLPG-polymerized liposome (500 μM) was incubated with 0−5 μM protein solution in 10 mM HEPES buffer, pH 7.4, containing 0.145 M NaCl, 10 mM $CaCl_2$, and 1 μM bovine serum albumin for 30 min at room

	1									10		51																		60										70
bpPLA$_2$	A	L	W	Q	F	**N**	**G**	M	I	**K**	C	C	Y	K	Q	A	**K**	K	L	D	S	C	K	**V**	L	**V**	D	N	P	Y	T								
ppPLA$_2$	A	L	W	Q	F	R	S	M	I	K	C	C	Y	R	D	A	K	N	L	D	S	C	K	F	L	V	D	N	P	Y	T								
hpPLA$_2$	A	V	W	Q	F	R	K	M	I	K	C	C	Y	D	Q	A	K	K	L	D	S	C	K	F	L	L	D	N	P	Y	T								

FIGURE 1: Sequence alignment of bovine, porcine, and human pancreatic PLA_2s. The amino-terminal 11 residues and residues 51−70 are shown. Amino acids in boldface characters indicate mutated residues.

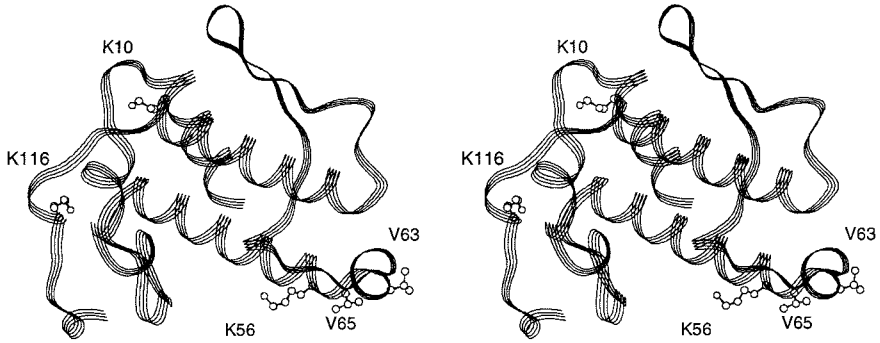

FIGURE 2: Stereo ribbon diagram of bovine pancreatic PLA_2 constructed from its crystal structure (*35*). The side chains of Lys-10, Lys-56, Val-63, Val-65, and Lys-116 are shown.

temperature. The mixtures (500 μL each) were then centrifuged for 15 min at 100000*g* and at 37 °C using a Sorvall RCM120EX microultracentrifuge equipped with S120AT3 rotor (Sorvall) to pellet polymerized liposomes. After centrifugation, the concentration of free enzyme ($[E]_f$) in the supernatant was determined by measuring the PLA_2 activity toward pyrene-PG/BLPG-polymerized mixed liposomes as described above. The bound PLA_2 concentration ($[E]_b$) was plotted as a function of $[E]_f$, and values of n and K_d were determined by nonlinear least-squares analysis of the $[E]_b$ versus $[E]_f$ plot using the standard Langmuir-type binding equation:

$$[E]_b = ([BLPG]_T/n)/(1 + K_d/[E]_f) \quad (1)$$

where $[BLPG]_T$ represents the total BLPG concentration. Equation 1 assumes that each enzyme binds independently to a site on the interface composed of n phospholipids and with a dissociation constant of K_d.

RESULTS

Characterization of Wild-Type and Mutants. To systematically analyze the effects of mutations on the interfacial binding of $bpPLA_2$, we measured three properties of mutants: enzyme activity toward diC_6PC monomers and toward pyrene-PG/BLPG-polymerized mixed liposomes and binding affinity for BLPG-polymerized liposomes. The first measurement would reveal whether the mutations disrupt the integrity of the active site of $bpPLA_2$ while the latter two sensitively detect changes in interfacial enzyme activity (*8*) and interfacial binding affinity (*11*, *13*, *19*), respectively. Also, we measured the CD spectra of mutants and determined their thermodynamic stability from guanidinium chloride-induced denaturation curves to determine whether the mutations led to the changes in secondary structure and in protein stability, respectively.

Properties of Amino-Terminal α*-Helix Mutants*. Many secretory PLA_2s including $hpPLA_2$ have a prominent cationic patch in the amino-terminal region, and the patch plays an essential role in their binding to anionic lipid surfaces (*20*−*22*). In contrast, $bpPLA_2$ contains only one cationic residue, Lys-10, in the amino-terminal α-helix (see Figures 1 and 2), and its contribution to interfacial binding is modest (see Table 1). Judging from the effects of their charge-reversal mutations on interfacial binding and activity, Lys-56 and Lys-116 make larger contributions than Lys-10 to the interfacial binding of $bpPLA_2$. To explore the possibility that the generation of a cationic patch in the amino-terminal region of $bpPLA_2$ might shift the location of its interfacial binding surface, we introduced cationic residues at positions 6 and/or 7 by N6R/G7K, N6R, and G7K mutations, respectively. These mutations were based on the amino acid sequences of $ppPLA_2$ and $hpPLA_2$ (see Figure 1). These mutations did not affect the protein stability and the secondary structure of $bpPLA_2$ as indicated by unaltered guanidinium chloride-induced denaturation curves and CD spectra of mutants (data not shown). Then, we further introduced the K56E mutation to these mutants, G7K/K56E and N6R/G7K/K56E, to see if the creation of a new cationic patch reduces the contribution of Lys-56 to total interfacial binding. First of all, all these mutants showed comparable activity toward diC_6PC, indicating lack of deleterious structural changes (Table 1). When the activity was measured using pyrene-PG/BLPG-polymerized mixed liposomes as a substrate, the effect of these extra cationic residues on the interfacial activity of $bpPLA_2$ was modest: i.e., N6R, G7K, and N6R/G7K showed 1.1-, 1.2-, and 2.5-fold increases in activity, respectively. As described in the preceding paper (*36*), the relative activity of mutants toward polymerized mixed liposomes can be estimated from their relative affinity for polymerized liposomes using the equation: $[E]_{bound}/[E]_{total} = 1/(1 + nK_d/[BLPG]_{total})$. Based on this estimation, the enhanced activity of the three mutants is in line with their improved affinity for BLPG-polymerized liposomes, i.e., 5-, 8-, and 15-fold increases for N6R, G7K, and N6R/G7K, respectively (see Figure 3 and Table 1). Thus, the generation of a cationic patch in the amino-terminal α-helix increases the population of liposome-bound $bpPLA_2$, thereby enhancing its overall interfacial activity. It does not seem to, however, change the interfacial binding mode of $bpPLA_2$ as the K56E mutation

Table 1: Kinetic and Interfacial Binding Properties of Bovine Pancreatic PLA_2 and Its Mutants

enzyme	$(k_{cat}/K_m)_{app}$[a] for diC_6PC monomers ($\times 10^2\ M^{-1}\ s^{-1}$)	$(k_{cat}/K_m)_{app}$[a] for pyrene-PG/BLPG-polymerized mixed liposomes		nK_d[b] for BLPG-polymerized liposomes (μM)
		$\times 10^3\ M^{-1}\ s^{-1}$	% activity	
wild-type	7 ± 1	1100 ± 200	100	40 ± 10
K10E	7 ± 2	230 ± 20	21	90 ± 15
K56E	11 ± 3[c]	15 ± 3	1.4[c]	450 ± 50
K116E	4 ± 1[d]	55 ± 9	5	450 ± 75
N6R	7 ± 1	1200 ± 100	110	8 ± 3
G7K	7 ± 3	1300 ± 200	120	5 ± 2
N6R/G7K	8 ± 1	2700 ± 300	250	3 ± 1
G7K/K56E	9 ± 1[c]	26 ± 2	2.4[c]	100 ± 15
N6R/G7K/ K56E	9 ± 1[c]	45 ± 3	4.1[c]	40 ± 10
Δ^{62-66}	8 ± 1	1200 ± 200	110	40 ± 10
Δ^{62-66}/K56E	9 ± 2[c]	400 ± 100	36[c]	40 ± 12
Δ^{62-66}/K116E	3 ± 1[d]	600 ± 200	55	41 ± 10
Δ^{62-66}/K10E	8 ± 1	40 ± 10	3.6	450 ± 50
V63F	6 ± 1	3700 ± 200	340	8 ± 4
V63F/K10E	6 ± 1	1100 ± 100	100	40 ± 15
V63F/K56E	10 ± 1[c]	700 ± 150	64[c]	20 ± 10
V63F/V65L	8 ± 1	1400 ± 200	130	25 ± 10
V63F/V65L/K10E	7 ± 1	50 ± 10	4.5	350 ± 50
V63F/V65L/K56E	9 ± 1[c]	450 ± 30	41[c]	50 ± 20

[a] The $(k_{cat}/K_m)_{app}$ values represent mean value $\pm$ SD determined from at least three measurements. [b] The nK_d values represent best-fit value $\pm$ SD determined from the nonlinear least-squares analyses of data. [c] Note that the K56E mutation modestly enhances the activity toward diC_6PC monomers because Lys-56 electrostatically repels the cationic choline head group. Also, this mutation reduces the activity toward polymerized mixed liposomes more significantly than expected from the decrease in interfacial affinity because Lys-56 favorably interacts with the PG head group (*8*). [d] The reduced activity of K116E mutants toward diC_6PC monomers was also seen with other pancreatic enzymes.[2]

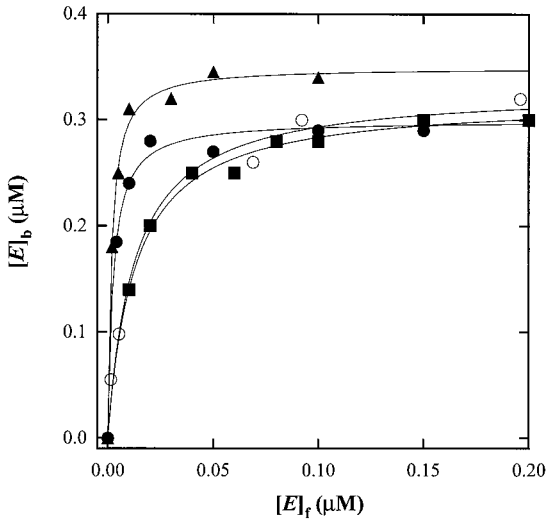

FIGURE 3: Binding isotherms of bovine pancreatic PLA_2 (○) and amino-terminal mutants, including N6R (●), N6R/G7K (▲), and N6R/G7K/K56E (■). The BLPG concentrations were 500 μM in 10 mM HEPES buffer, pH 7.4, containing 0.145 M NaCl and 10 mM $CaCl_2$. The solid lines indicate the theoretical curves constructed using eq 1 with the n and K_d values determined from the nonlinear least-squares analyses.

resulted in 50-fold and 60-fold decreases in the activity of G7K and N6R/G7K, respectively. These effects are comparable with the effect of the same mutation on the wild-type (70-fold). Also, the K56E mutation reduced the affinity of G7K and N6R/G7K for BLPG-polymerized liposomes by 12- and 14-fold, respectively (Table 1). Note that the K56E mutation decreases the PLA_2 activity toward pyrene-PG/BLPG-polymerized mixed liposomes more significantly than its affinity for BLPG-polymerized liposomes because Lys-56 is involved in both interfacial binding and substrate binding (*8*). Taken together, these data indicate that the lack of a cationic patch in the amino-terminal α-helix of $bpPLA_2$ is not responsible for its unique interfacial binding mode.

Properties of Δ^{62-66} Mutants. Mammalian pancreatic PLA_2s contain a unique sequence extension (residues 62−66) in a loop connecting the α-helix containing Lys-56 to the β-wing. A molecular dynamics calculation showed that this pancreatic loop region of $bpPLA_2$ is highly flexible (*23*). To explore the possibility that the flexibility of the pancreatic loop is essential for the interaction of its adjacent Lys-56 with anionic interfaces, we prepared a mutant lacking residues 62−66 (Δ^{62-66}) and measured the effect of the K56E mutation (i.e., Δ^{62-66}/K56E) on the interfacial affinity and activity of this mutant. We also made two additional mutants, Δ^{62-66}/K10E and Δ^{62-66}/K116E, to see if the deletion of the pancreatic loop changes the interfacial binding mode of $bpPLA_2$. Previously, Kuipers et al. (*24*) made a mutant of $ppPLA_2$ lacking residues 62−66, which showed essentially the same crystal structure as $ppPLA_2$ except for the modified loop region. The bovine Δ^{62-66}, Δ^{62-66}/K10E, Δ^{62-66}/K56E, and Δ^{62-66}/K116E showed indistinguishable CD spectra that were only slightly different from that of wild-type, indicating lack of major changes in secondary structure caused by the deletion of the pancreatic loop (Figure 4). The thermodynamic stability of these mutants was also similar to that of wild-type (Figure 5): $\Delta G_{fold} = -12.6 \pm 0.2$ kcal/mol at 23 °C and $m = 1.7 \pm 0.1$ kcal $mol^{-1}\ M^{-1}$. The porcine deletion mutant showed higher activity [i.e., 4 times higher $(k_{cat}/K_m)_{app}$] than wild-type toward zwitterionic diC_8PC micelles but lower activity toward anionic micelles (*24*). The bovine Δ^{62-66} mutant showed different kinetic behaviors: It was only modestly more active than wild-type toward zwitterionic diC_6PC monomers (14% increase; see Table 1) and diC_8PC micelles [$(k_{cat}/K_m)_{app} = 2.0 \times 10^5\ M^{-1}\ s^{-1}$; 50% increase] and showed no decrease in activity toward anionic pyrene-PG/BLPG-polymerized mixed liposomes (Table 1). Also, Δ^{62-66} had liposome binding affinity comparable with that of wild-type. Importantly, the effects of K10E, K56E, and K116E mutations on the interfacial activity and affinity of

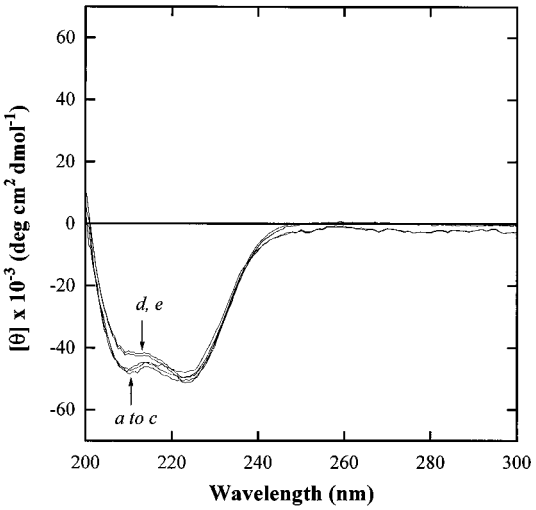

FIGURE 4: Circular dichroism spectra of bovine pancreatic PLA_2 (a), V63F (b), V63F/V65L (c), Δ^{62-66} (d), and Δ^{62-66}/K56E (e). The protein concentrations were 25 μM in 0.1 M phosphate buffer, pH 7.4. Other mutants of Δ^{62-66} also have identical spectra.

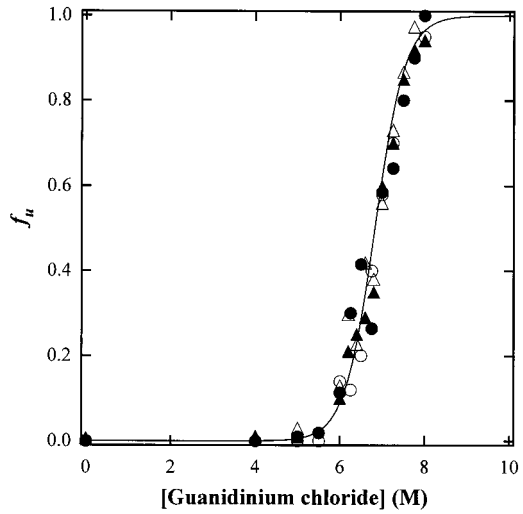

FIGURE 5: Guanidinium chloride-induced unfolding of bovine pancreatic PLA_2 (○), V63F (●), V63F/V65L (△), and Δ^{62-66} (▲) at 23 °C. The protein concentrations were 25 μM in 0.1 M phosphate buffer, pH 7.4. The f_u values were calculated from θ_{222} values as described under Materials and Methods. A theoretical curve was constructed for wild-type using the ΔG_{fold} and m values determined from the nonlinear least-squares analysis of data. All the mutants have essentially the same ΔG_{fold} and m values.

this deletion mutant were completely different from those seen for wild-type. First, the K56E mutation reduced the activity of the bovine Δ^{62-66} toward pyrene-PG/BLPG-polymerized mixed liposomes only 3 times, which was in striking contrast to the large effect (70-fold) of the same mutation on wild-type. Taking into account the involvement of Lys-56 in substrate binding, this low extent of rate decrease suggested essentially no reduction in interfacial binding. Second, the K116E mutation which led to a 20-fold decrease in the wild-type activity reduced the activity of Δ^{62-66} by half. Note that the K116E mutation also decreased the activity toward diC_6PC monomers to a comparable extent and that this negative effect on the catalytic efficiency of the enzyme was also seen with $hpPLA_2$ and $ppPLA_2$[2]. Thus, the net effect of the mutation on interfacial affinity should be negligible. Third, the K10E

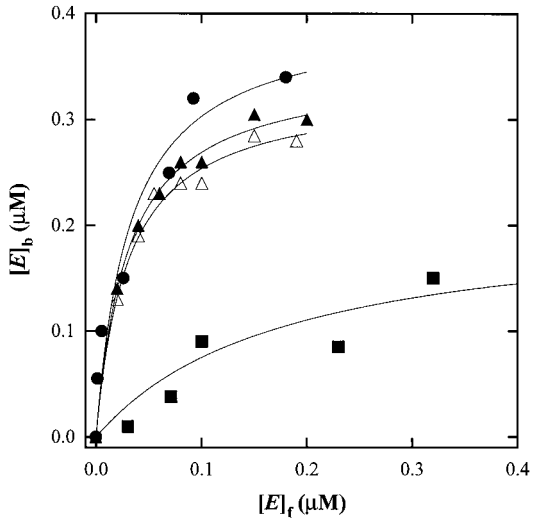

FIGURE 6: Binding isotherms of pancreatic loop mutants, including Δ^{62-66} (●), Δ^{62-66}/K10E (■), Δ^{62-66}/K56E (△), and Δ^{62-66}/K116E (▲). The experimental conditions and the method for calculation of binding parameters are the same as described for Figure 3.

mutation caused a 30-fold decrease in the activity of Δ^{62-66} toward pyrene-PG/BLPG-polymerized mixed liposomes. This large decrease in activity was not due to the loss of catalytic efficiency of the enzyme because Δ^{62-66}/K10E was as active as Δ^{62-66} toward diC_6PC monomers (Table 1). Finally, the relative liposome affinity of these mutants was in accordance with their relative activity toward polymerized mixed liposomes (see Figure 6 and Table 1). Δ^{62-66}/K10E showed 12-fold lower affinity for BLPG-polymerized liposomes than Δ^{62-66} whereas Δ^{62-66}/K56E and Δ^{62-66}/K116E exhibited liposome affinity comparable with that of Δ^{62-66}. Thus, although the pancreatic loop is not essential for the structure, stability, and activity of $bpPLA_2$, the deletion of the loop alters its interfacial binding mode in such a way that the amino-terminal Lys-10 plays a more direct role. Taken together, these results point to the importance of the pancreatic loop of $bpPLA_2$ in determining its interfacial binding mode.

Properties of Pancreatic Loop Mutants. To pinpoint the amino acid(s) in the pancreatic loop of $bpPLA_2$ that determine(s) its unique liposome binding mode, we prepared two additional mutants, V63F and V63F/V65L. As shown in Figure 1, V63F and V63F/V65L mutations would convert $bpPLA_2$ into $ppPLA_2$- and $hpPLA_2$-like structures, respectively. It was shown that a conservative substitution in position 63 led to a large conformational difference between $bpPLA_2$ and $ppPLA_2$ in the pancreatic loop region (*25*). Although the tertiary structure of $hpPLA_2$ is not available yet, it is also possible that the Val to Leu substitution in position 65 of $hpPLA_2$ causes further variations in the pancreatic loop conformation. As shown in Figure 4, CD spectra of wild-type, V63F, and V63F/V65L were indistinguishable, showing that potential changes in the loop conformation did not alter the secondary structure of $bpPLA_2$. Also, essentially identical guanidinium chloride-induced denaturation curves of wild-type and the mutants indicate that the mutations did not affect the protein stability (Figure 5). We previously showed that toward pyrene-PG/BLPG-

[2] See the accompanying paper (*36*).

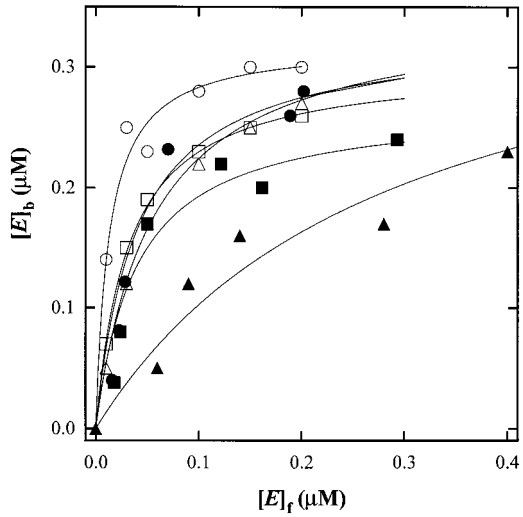

FIGURE 7: Binding isotherms of pancreatic loop mutants including V63F (○), V63F/K10E (△), V63F/K56E (□), V63F/V65L (●), V63F/V65L/K10E (▲), and V63F/V65L/K56E (■). The experimental conditions and the method for calculation of binding parameters are the same as described for Figure 3.

polymerized mixed liposomes, $ppPLA_2$ and $hpPLA_2$ are ca. 5 times and 1.5-fold more active than $bpPLA_2$, respectively (*26*). Interestingly, V63F and V63F/V65L, whose activity toward diC_6PC monomers is similar to that of wild-type, showed 3.4-fold and 1.3-fold higher activity than wild-type toward pyrene-PG/BLPG-polymerized mixed liposomes. This suggested that the residues in positions 63 and 65 might be important for the characteristic kinetic behavior of these pancreatic PLA_2s. The nK_d values for the liposome binding of V63F and V63F/V65L (see Figure 7 and Table 1) indicate that the enhanced activity of these mutants derives mainly from their higher interfacial affinity. To see if the two mutants and wild-type have different interfacial binding modes, we measured the effects of K10E and K56E mutations on the interfacial properties of the mutants. All these mutants showed the expected activity toward diC_6PC monomers, indicating lack of deleterious structural changes. For V63F, the K10E and K56E mutations caused 3.4-fold and 5.3-fold drops in activity toward pyrene-PG/BLPG-polymerized mixed liposomes, respectively. Also, decreases in liposome affinity were 5-fold and 2.5-fold for K10E and K56E, respectively, which was again in line with the changes in interfacial activity. Together, these data signal a significant change in the interfacial binding mode of $bpPLA_2$ caused by the V63F mutation in that Lys-56 is no longer a critical IBS residue. The change in interfacial binding mode was even more pronounced for V63F/V65L. For this mutant, the additional K10E mutation resulted in a 25-fold decrease in the activity toward liposomes and a 10-fold reduction in liposome affinity. In contrast, the decrease in interfacial affinity by the K56E mutation was only 2-fold. These effects are strikingly similar to the effects of the same mutations on the properties of $hpPLA_2$[2]. Thus, these results indicate that the V63F/V65L mutations effectively change the interfacial binding mode of $bpPLA_2$ to that of $hpPLA_2$. Taken together, it is evident that Val-63 and Val-65 of $bpPLA_2$ are the structural determinant of its unique interfacial binding mode and that relatively conservative substitutions at these positions result in large changes in the interfacial binding mode.

DISCUSSION

Most secretory PLA_2s prefer anionic phospholipid aggregates, such as phosphatidylglycerol (PG) liposomes, to electrically neutral ones, such as phosphatidylcholine (PC) liposomes. Our structure−function studies of different secretory PLA_2s have shown that their activity toward anionic interfaces depends on specific surface cationic residues and that the arrangement of these residues varies with the type of PLA_2s (*8, 10, 11*). The present report describes an extensive structure−function study of $bpPLA_2$ which identifies the structural determinant of its unique interfacial binding mode in which spatially separated Lys-56 and Lys-116 play essential roles (*8*).

A Cationic Cluster in the Amino-Terminal α-Helix. It has been shown that surface cationic patches of secretory PLA_2s, most notably snake venom PLA_2s, are responsible for their diverse pharmacological activities (*27*). Many secretory PLA_2s contain a cluster of cationic residues in their amino-terminal region that is generally thought to be a part of the interfacial binding surface (*10, 28*). In particular, cationic residues in positions 7 and 10 of PLA_2s have been shown to be important in their interactions with anionic interfaces (*11, 20*−*22, 29*−*32*). The distribution of cationic residues in the amino-terminal α-helix of pancreatic PLA_2s varies considerably. For instance, all but bovine PLA_2 have Arg at position 6 whereas all but equine PLA_2 contain Lys at position 10. Also, only human PLA_2 has cationic Lys at position 7. This raises the possibility that the different distribution of amino-terminal cationic residues among pancreatic enzymes might cause them to interact with anionic interfaces in different modes. Our results suggest otherwise. The introduction of two extra cationic residues by the N6R/G7K mutation converts $bpPLA_2$ into a $hpPLA_2$-like form containing three cationic residues on the same face of the amino-terminal α-helix. Yet, N6R/G7K behaves more like $bpPLA_2$ than like $hpPLA_2$ in that the K56E mutation has a large effect on its binding to anionic liposomes. The significant increase in the interfacial affinity of $hpPLA_2$ by the introduction of the amino-terminal cationic residues suggests, however, that in the course of interfacial catalysis of $bpPLA_2$ the amino-terminal α-helix makes contact with anionic lipid surfaces.

Lys-56 and Pancreatic Loop. The largest structural difference among various secretory PLA_2s is found in the surface loop connecting the *β*-wing to the long α-helix containing the catalytic residue His-48. When compared with group II secretory PLA_2s, group I PLA_2s from elapid and hydrophid venom and mammalian pancreas have a three amino acid insertion at residues 54−56, the so-called elapid loop. In particular, mammalian pancreatic PLA_2s (group Ib) invariably contain Lys at position 56 and have an additional five amino acid insertion at residues 62−66 (pancreatic loop). The X-ray structure and kinetic properties of the $ppPLA_2$ mutant lacking the pancreatic loop indicated that the loop does not have any significant structural role but might be involved in binding to aggregated substrates (*24*). Our CD and stability measurements of bovine Δ^{62-66} also indicate that the pancreatic loop is not important for its structure and stability. Kinetic and binding properties of Δ^{62-66} show that the pancreatic loop of $bpPLA_2$ is not directly involved in binding to aggregated substrates per se but might be involved

in properly orienting Lys-56 at the anionic lipid surface. The different effects of the loop deletion on the enzyme activity of $bpPLA_2$ and $ppPLA_2$ might derive from the structural differences between the two enzymes in the pancreatic loop, caused by the substitution at position 63 (Figure 1 and see below) (*25*). Also, the porcine loop-deletion mutant has two additional mutations at positions 60 and 66 (*24*). The finding that neither Lys-56 nor Lys-116 is essential for the interfacial binding of Δ^{62-66} suggests that the molecular orientation of $bpPLA_2$ optimal for the interaction of Lys-56 with the anionic interface also brings the side chain of Lys-116 close to the interface. As a result, the pancreatic loop appears to govern the actions of the two critical interfacial binding residues of $bpPLA_2$ at the lipid surface. The low interfacial activity and affinity observed for Δ^{62-66}/K10E clearly indicates that in the absence of the pancreatic loop, $bpPLA_2$ has an altered interfacial binding mode in which the amino-terminal α-helix mainly serves as an anchor to the anionic lipid surface. Apparently, this interfacial binding mode, which is similar to that of $hpPLA_2$, is as efficient as the original interfacial binding mode in that wild-type and Δ^{62-66} have the same activity toward micelles and polymerized mixed liposomes. Thus, the role of the pancreatic loop is not to enhance the overall activity of $bpPLA_2$ but to orient the enzyme in a specific manner at the lipid surface. The functional consequences and the physiological significance of this orientation effect remain to be elucidated.

The X-ray structure of $bpPLA_2$ shows that the inward location of the Lys-56 side chain creates a cationic "groove" on the putative interfacial binding surface (see Figure 2) (*33*). The C_α atom of Lys-56 is located within 11 Å from the C_α atoms of residues 62−66 (*34*). The time-averaged restrained molecular dynamics refinement of the X-ray structure of $bpPLA_2$ showed that its pancreatic loop is highly mobile (*23*). Based on this structural information, it is tempting to propose that the high flexibility of the pancreatic loop allows the side chain of Lys-56 to move outward to make optimal electrostatic contact with the anionic lipid surface. It should be noted that among characterized mammalian pancreatic PLA_2s only $bpPLA_2$ has Val in position 63 (all other have Phe). In position 65, on the other hand, bovine, porcine, and equine PLA_2s have Val and others have larger Leu or Ile. Both Val-63 and Val-65 of $bpPLA_2$ are solvent-exposed (see Figure 2) (*33*) whereas the bulkier Phe-63 of $ppPLA_2$ is buried inside to avoid energetically unfavorable contact with water (*25*). This internal packing of the hydrophobic side chain would reduce the flexibility of the pancreatic loop. Thus, the V63F/V65L mutant of $bpPLA_2$ as well as $hpPLA_2$ should have less flexible pancreatic loops. The finding that Lys-56 is no longer critical for the interfacial binding of the bovine V63F and V63F/V65L mutants supports the notion that the flexibility of the pancreatic loop of $bpPLA_2$ is essential for the interfacial binding of Lys-56. Thus, relatively conservative variations in positions 63 and 65 of the pancreatic loop greatly influence the interfacial binding mode of pancreatic PLA_2s, presumably by affecting the flexibility of the loop. Finally, the striking similarity between the bovine V63F/V65L mutant and $hpPLA_2$ shows that one can effectively convert $bpPLA_2$ to $hpPLA_2$ by the point mutations at the key locations in the pancreatic loop. The similarity between the bovine V63F mutant and $ppPLA_2$, albeit less obvious, also supports this notion. Together, the present study demonstrates how minor structural differences among secretory PLA_2s can lead to distinct interfacial binding modes.

ACKNOWLEDGMENT

We thank Edward T. Yoon for preparing polymerized (mixed) liposomes.

REFERENCES

1. Mayer, R. J., and Marshall, L. A. (1993) *FASEB J. 7*, 339−348.
2. Kudo, I., Murakami, M., Hara, S., and Inoue, K. (1993) *Biochim. Biophys. Acta 1170*, 217−231.
3. Roberts, M. F. (1996) *FASEB J. 10*, 1159−1172.
4. Scott, D. L., and Sigler, P. B. (1994) *Adv. Protein Chem. 45*, 53−88.
5. Dennis, E. A. (1994) *J. Biol. Chem. 269*, 13057−13060.
6. Dennis, E. A. (1997) *Trends Biochem. Sci. 22*, 1−2.
7. Scott, D. L., White, S. P., Otwinowski, Z., Gelb, M. H., and Sigler, P. B. (1990) *Science 250*, 1541−1546.
8. Dua, R., Wu, S.-K., and Cho, W. (1995) *J. Biol. Chem. 270*, 263−268.
9. Lee, B.-I., Yoon, E. T., and Cho, W. (1996) *Biochemistry 35*, 4231−4240.
10. Han, S.-K., Yoon, E. T., Scott, D. L., Sigler, P. B., and Cho, W. (1997) *J. Biol. Chem. 272*, 3573−3582.
11. Snitko, Y., Koduri, R., Han, S.-K., Othman, R., Baker, S. F., Molini, B. J., Wilton, D. C., Gelb, M. H., and Cho, W. (1997) *Biochemistry 36*, 14325−14333.
12. Ghomashchi, F., Lin, Y., Hixon, M. S., Yu, B. Z., Annand, R., Jain, M. K., and Gelb, M. H. (1998) *Biochemistry 37*, 6697−6710.
13. Wu, S.-K., and Cho, W. (1993) *Biochemistry 32*, 13902−13908.
14. Kates, M. (1986) *Techniques of Lipidology*, 2nd ed., Elsevier, Amsterdam.
15. Nakamaye, K., and Eckstein, F. (1986) *Nucleic Acids Res. 14*, 9679−9698.
16. Deng, T., Noel, J. P., and Tsai, M.-D. (1990) *Gene 93*, 229−234.
17. Pace, C. N. (1986) *Methods Enzymol. 131*, 266−280.
18. Santoro, M. M., and Bolen, D. W. (1988) *Biochemistry 27*, 8063−8068.
19. Wu, S.-K., and Cho, W. (1994) *Anal. Biochem. 221*, 152−159.
20. Dua, R., and Cho, W. (1994) *Eur. J. Biochem. 221*, 481−490.
21. Cho, W., Tomasseli, A. G., Heinrikson, R. L., and Kézdy, F. J. (1988) *J. Biol. Chem. 263*, 11237−11241.
22. Shen, Z., Wu, S.-K., and Cho, W. (1994) *Biochemistry 33*, 11598−11607.
23. Gros, P., van Gunsteren, W. F., and Hol, W. G. J. (1990) *Science 249*, 1149−1152.
24. Kuipers, O. P., Thunnissen, M. M. G. M., De Geus, P., Dijkstra, B. W., Drenth, J., Verheij, H. M., and De Haas, G. H. (1989) *Science 244*, 82−85.
25. Dijkstra, B. W., Renetseder, R., Kalk, K. H., Hol, W. G. J., and Drenth, J. (1983) *J. Mol. Biol. 168*, 163−179.
26. Han, S.-K., Lee, B.-I., and Cho, W. (1997) *Biochim. Biophys. Acta 1346*, 185−192.
27. Kini, R. M., and Evans, H. J. (1987) *J. Biol. Chem. 262*, 14402−14407.
28. Jain, M. K., and Berg, O. G. (1989) *Biochim. Biophys. Acta 1002*, 127−156.
29. Weiss, J., Wright, G., Bekkers, A. C. A. P. A., van den Bergh, C. J., and Verheij, H. M. (1991) *J. Biol. Chem. 266*, 4162−4167.
30. Weiss, J., Inada, M., Elsbach, P., and Crowl, R. M. (1994) *J. Biol. Chem. 269*, 26331−26337.
31. Inada, M., Crowl, R. M., Bekkers, A. C. A. P. A., Verheij, H. M., and Weiss, J. (1994) *J. Biol. Chem. 269*, 26338−26343.

32. Shen, Z., and Cho, W. (1995) *J. Lipid Res. 36*, 1147−1151.
33. Dijkstra, B. W., Drenth, J., and Kalk, K. H. (1981) *Nature 289*, 604−606.
34. Dijkstra, B. W., Kalk, K. H., Hol, W. G. J., and Drenth, J. (1981) *J. Mol. Biol. 147*, 97−123.
35. Dijkstra, B. W., Drenth, J., Kalk, K. H., and Vandermaelen, P. J. (1978) *J. Mol. Biol. 124*, 53−60.
36. Snitko, Y., Han, S. K., Lee, B. I., and Cho, W. (1999) *Biochemistry 38*, 7803−7810.

BI9906017